



HAL
open science

Relationships between growth, growth response to nutrient supply, and ion content using a recombinant inbred line population in *Arabidopsis*

Aina E. Prinzenberg, Hugues Barbier, David E. Salt, Benjamin Stich,
Matthieu Reymond

► To cite this version:

Aina E. Prinzenberg, Hugues Barbier, David E. Salt, Benjamin Stich, Matthieu Reymond. Relationships between growth, growth response to nutrient supply, and ion content using a recombinant inbred line population in *Arabidopsis*. *Plant Physiology*, 2010, 154 (3), pp.1361-1371. 10.1104/pp.110.161398 . hal-01203874

HAL Id: hal-01203874

<https://hal.science/hal-01203874>

Submitted on 31 May 2020

HAL is a multi-disciplinary open access archive for the deposit and dissemination of scientific research documents, whether they are published or not. The documents may come from teaching and research institutions in France or abroad, or from public or private research centers.

L'archive ouverte pluridisciplinaire **HAL**, est destinée au dépôt et à la diffusion de documents scientifiques de niveau recherche, publiés ou non, émanant des établissements d'enseignement et de recherche français ou étrangers, des laboratoires publics ou privés.

Relationships between Growth, Growth Response to Nutrient Supply, and Ion Content Using a Recombinant Inbred Line Population in Arabidopsis^{1[W][OA]}

Aina E. Prinzenberg², Hugues Barbier², David E. Salt, Benjamin Stich, and Matthieu Reymond*

Department of Plant Breeding and Genetics, Max Planck Institute for Plant Breeding Research, 50829 Cologne, Germany (A.E.P., B.S., M.R.); Institut de Biologie Moléculaire des Plantes du CNRS, Institut de Biologie Moléculaire des Plantes-CNRS-UPR2357, 67084 Strasbourg, France (H.B.); Center for Plant Environmental Stress Physiology, Horticulture and Landscape Architecture Department, Purdue University, West Lafayette, Indiana 47907 (D.E.S.); and Institut Jean-Pierre Bourgin, UMR1318 INRA-AgroParisTech, INRA Centre de Versailles-Grignon, 78026 Versailles cedex, France (M.R.)

Growth is an integrative trait that responds to environmental factors and is crucial for plant fitness. A major environmental factor influencing plant growth is nutrient supply. In order to explore this relationship further, we quantified growth-related traits, ion content, and other biochemical traits (protein, hexose, and chlorophyll contents) of a recombinant inbred line population of Arabidopsis (*Arabidopsis thaliana*) grown on different levels of potassium and phosphate. Performing an all subsets multiple regression analyses revealed a link between growth-related traits and mineral nutrient content. Based on our results, up to 85% of growth variation can be explained by variation in ion content, highlighting the importance of ionomics for a broader understanding of plant growth. In addition, quantitative trait loci (QTLs) were detected for growth-related traits, ion content, further biochemical traits, and their responses to reduced supplies of potassium or phosphate. Colocalization of these QTLs is explored, and candidate genes are discussed. A QTL for rosette weight response to reduced potassium supply was identified on the bottom of chromosome 5, and its effects were validated using selected near isogenic lines. These lines retained over 20% more rosette weight in reduced potassium supply, accompanied by an increase in potassium content in their leaves.

Plants in natural environments face abiotic constraints limiting growth and ultimately affecting their fitness. In response to such constraints, flowering time (Korves et al., 2007) and seed dormancy (Donohue et al., 2005) as well as vegetative growth (Barto and Cipollini, 2005; Milla et al., 2009) are the main traits controlling fitness (for review, see Alonso-Blanco et al., 2009). These traits are under the control of complex networks integrating genetic (G) and environmental (E) factors as well as their interaction (G × E). Due to the implications for food and renewable energy sources, dissecting the genetic architecture that underlies plant growth is becoming a priority for plant science (Rengel and Damon, 2008; Carroll and Somerville, 2009; Gilbert, 2009).

Plant growth is highly dependent on mineral nutrient uptake (Clarkson, 1980; Sinclair, 1992). Minerals can be distinguished into two categories based on the amount required by plants: micronutrients, which are found in relatively small amounts in the plant (such as copper and iron), and macronutrients, which constitute between 1,000 and 15,000 $\mu\text{g g}^{-1}$ plant dry weight (such as potassium and phosphate; Marschner, 1995; Buchanan et al., 2002). Phosphate is an important structural and signaling molecule with an essential role in photosynthesis, energy conservation, and carbon metabolism. Its deficiency leads to a reduction of growth and an increase of pathogen susceptibility (Marschner, 1995; Williamson et al., 2001; Abel et al., 2002; López-Bucio et al., 2005; Poirier and Bucher, 2008; Vijayraghavan and Soole, 2010). Potassium is not incorporated into any organic substances but acts as the major osmoticum of the cell, controlling cell expansion, plasma membrane potential and transport, pH value, and many other catalytic processes (Maathuis and Sanders, 1996; Armengaud et al., 2004; Christian et al., 2006; Di Cera, 2006). Potassium deficiency leads to reduced plant growth, a loss of turgor, increased susceptibility to cold stress and pathogens, and the development of chlorosis and necrosis (Marschner, 1995; Véry and Sentenac, 2003; Ashley et al., 2006; Amtmann et al., 2008). To cope with changes in nutrient availability, plants have evolved different

¹ This work was supported by the Max Planck Society and the U.S. National Institutes of Health (grant no. GM078536 to D.E.S.).

² These authors contributed equally to the article.

* Corresponding author; e-mail matthieu.reymond@versailles.inra.fr.

The author responsible for distribution of materials integral to the findings presented in this article in accordance with the policy described in the Instructions for Authors (www.plantphysiol.org) is: Matthieu Reymond (matthieu.reymond@versailles.inra.fr).

^[W] The online version of this article contains Web-only data.

^[OA] Open Access articles can be viewed online without a subscription.

www.plantphysiol.org/cgi/doi/10.1104/pp.110.161398

mechanisms of adaptation, such as changes in ion transporter expression and activity (Ashley et al., 2006; Jung et al., 2009), morphological changes, such as an increase in root growth to explore more soil volume (Marschner, 1995; Shirvani et al., 2001; Jiang et al., 2007; Jordan-Meille and Pellerin, 2008), or acidification of the surrounding soil in order to mobilize more mineral nutrients (for review, see Ryan et al., 2001). Although these adaptations are well known, the mechanisms involved in sensing and signaling low mineral nutrient status are less well understood, despite significant progress in this area being made (Doerner, 2008; Jung et al., 2009; Luan et al., 2009; Wang and Wu, 2010).

One approach to identify genes that are involved in plant responses to environmental factors is to perform a quantitative trait locus (QTL) analysis on a mapping population grown in contrasting environments, allowing the identification of QTL-environment (QTL \times E) interactions. Some QTLs for growth-related traits in response to environmental changes were cloned already. For example, the differential response of root growth of some *Arabidopsis* (*Arabidopsis thaliana*) accessions to phosphate starvation led to the identification of allelic differences responsible for this phenotype (Reymond et al., 2006; Svistoonoff et al., 2007). Other studies have identified QTLs for shoot dry matter under changing nitrogen supply (Rauh et al., 2002; Loudet et al., 2003). In parallel to natural variation for growth, natural variation for ion content has also been reported. In *Arabidopsis*, considerable variation in the content of mineral nutrients exists both in seeds (Vreugdenhil et al., 2004; Waters and Grusak, 2008) and in leaves (Harada and Leigh, 2006; Rus et al., 2006; Baxter et al., 2008a; Morrissey et al., 2009). Furthermore, changes in mineral nutrient homeostasis have also been reported to be associated with characteristic multivariate changes in the leaf ionome, the mineral nutrient and trace element composition of an organism or an organ (Baxter et al., 2008b). Due to higher throughput and lower costs, such “omics” analyses examining alterations of large numbers of certain molecules at once have recently become available for mapping purposes. Some QTL studies have linked the variations of these omics data to variation of growth or other physiological traits. For instance, Meyer et al. (2007) and Schauer et al. (2008) linked plant growth or morphological traits to a synergistic network of metabolomic compounds in *Arabidopsis* and tomato (*Solanum lycopersicum*), respectively. In addition, Sulpice et al. (2009) associated differences in growth with starch content using a set of *Arabidopsis* accessions. Compiling the importance of ions in the process of cell division (Lai et al., 2007; Sano et al., 2007) or cell expansion (Phillippar et al., 1999; Elumalai et al., 2002), ionomics appears to be a major unexplored field for understanding growth.

In this study, we focus on variation in plant growth, the root and leaf ionomes, and their response to varying supplies of potassium and phosphate. Study-

ing variations for these traits among recombinant inbred lines (RILs) in *Arabidopsis* enabled us to detect QTL and QTL \times E interactions for all of these traits. To understand the observed variation in plant growth, predictors that explained a high percentage of variation of growth-related traits have been selected especially among the root and leaf ionomes. The colocalization between growth-related trait QTLs and QTLs for their predictors allowed us to point out genetic regions of possible causality. In addition, the effect of a growth-response QTL on reduced potassium supply was validated with selected near isogenic lines (NILs) that maintained a higher rosette weight when grown in reduced potassium supply. This growth advantage went along with significant changes in ion contents that further emphasize the impact of the ionome in plant growth variations.

RESULTS

Correlations between the Quantified Growth-Related Traits

Selected lines of the Landsberg *erecta* (*Ler*) \times Kashmir-2 (Kas-2) RIL population (El-Lithy et al., 2006) were grown under different nutrient regimes (control [C], reduced potassium [K-], and reduced phosphate [P-] media) using a hydroponic cultivation system (Tocquin et al., 2003). Different growth-related traits were quantified, such as rosette weight, root weight, and root length of plants, 32 d after transfer to the growth cabinet (DAT; see “Materials and Methods”). In addition, the relative growth rate (RGR; see “Materials and Methods”) of the projected rosette area was quantified between 7 and 22 DAT. Rosette weight and root weight were strongly and significantly correlated (r values between 0.79 and 0.89; Table I), as were, to a lesser extent, root weight and root length (r values between 0.32 and 0.4; Table I). No significant correlations were observed between rosette weight and root length, nor between root length and RGR, in any of the nutrient regimes. The correlations between rosette weight, root weight, and root length were not affected by nutrient regime (Table I). Rosette weight and root weight were correlated with RGR (r values between 0.46 and 0.6 in C and P-), and these correlations were less pronounced in the K- regime ($r = 0.29$ and 0.2).

Linking the Variation of Growth-Related Traits and the Variation of Ionomic Traits

A multiple regression analysis (all subset multiple regression; see “Materials and Methods”) was performed to examine to what extent the variation of the growth-related traits can be explained by that of chlorophyll, protein, and hexose content, ionomics (of the rosette [$_{rs}$] or the root [$_{rt}$]), and leaf number (leaf number at 22 DAT [L22] or leaf number at 32 DAT [L32]). Hence, a set of predictors were selected that significantly explained the variation of the growth-

Table I. Correlation of all growth-related traits

The Pearson's correlation coefficients (r) and P values for the correlation of all growth-related traits, rosette weight, root weight, root length, and RGR, are reported for each treatment (C, K-, and P-).

Trait	Treatment	Rosette Weight		Root Weight		Root Length	
		r	P	r	P	r	P
Root weight (g)	C	0.79	3.1E-29				
	K-	0.89	4.9E-46				
	P-	0.86	7.8E-40				
Root length (cm)	C	0.15	9.6E-02	0.40	2.9E-06		
	K-	0.20	2.0E-02	0.38	1.2E-05		
	P-	0.22	1.4E-02	0.32	2.5E-04		
RGR (d^{-1})	C	0.52	2.1E-10	0.46	4.3E-08	0.11	2.3E-01
	K-	0.29	7.6E-04	0.20	2.0E-02	-0.07	4.2E-01
	P-	0.55	2.4E-11	0.60	1.0E-13	0.13	1.4E-01

related traits or the variation of the growth responses to the different mineral nutrient regimes (Table II). All together, 10 to 13 predictors and their correlations (Table II; Supplemental Fig. S1) explained from 66.2% to 84.7% of the rosette weight and root weight variance in the different nutrient regimes (C, K-, and P-). RGR and root length were explained by four to 13 predictors, which together explained between 40.8%, and 55.3% (Table II). A small percentage of the variance in the growth-related traits for response to nutrient supply (change in the percentage of a trait in the reduced nutrient supply compared with the control [Kresp and Presp]) was explained by predictors. However, this is not the case for the response of root length to the low-phosphate regime (Presp), where a combination of 13 predictors explained up to 54.1% of the variation of this trait.

The previously described correlations between the different growth-related traits (Table I) are reflected in the number of common predictors. Root weight and rosette weight were highly correlated and shared the highest number of predictors (six for C, eight for K-, and seven for P-; Table II). The correlations between root length and rosette weight, respectively, RGR and root length were lower than between root weight and rosette weight, as were the number of common predictors. Furthermore, root length was explained by few predictors, most of which also explained the variation of root weight, which is in accordance with the correlation between these traits (Table I).

QTL Mapping of Growth-Related Traits

Fifty-six QTLs involved in the variation of all growth-related traits were detected in all three nutrient regimes. For each QTL, the presence of a significant environmental interaction ($Q \times E$) was then tested against the control condition, for QTLs detected in K- and P- and against K- and P- for the QTL detected in the control condition (see "Materials and Methods"). These QTLs are presented according to their location in 31 bins (comprising 15 centimorgan [cM] of the genetic map from the Kas-2 \times Ler map-

ping population) along the five chromosomes (1-1 to 1-7 for chromosome 1, 2-1 to 2-6 for chromosome 2, 3-1 to 3-6 for chromosome 3, 4-1 to 4-5 for chromosome 4, and 5-1 to 5-7 for chromosome 5; Fig. 1). The 56 QTLs for growth-related traits explained between 3% and 22.3% of the phenotypic variation of the traits (Supplemental Table S1). For one-quarter of these QTLs, their effect was significantly different between nutrient regimes ($G \times E$; Fig. 1). In addition, we identified three QTLs for the responses of growth-related traits to the reduced nutrient regimes (Presp, root length and RGR; Kresp, rosette weight). The response QTL to reduced potassium supply (Fig. 1B, bin 5-5) explained 9.3% of the variation of the rosette weight response, with the *Ler* alleles increasing the rosette weight response (Supplemental Table S1). This is the only QTL detected for the growth response to K- among the growth-related traits quantified.

In accordance with the correlations between the quantified growth-related traits (Table I), colocalizations of QTLs of different growth-related traits have been observed: QTLs for root weight and root length were detected in all treatments on the top of chromosome 1 (Fig. 1, bin 1-3). At this position is a $G \times E$ effect for the root length QTL between C and P-, and accordingly, a QTL for the response of root length to P- has also been detected there. Another example of colocalizing QTLs of correlated growth-related traits is on chromosome 2 (in the vicinity of the marker *Erecta*, bin 2-4): QTLs of rosette and root weight were detected in all nutrient regimes.

QTL Mapping of Chlorophyll, Protein, Hexose, Ionomic Traits, and Leaf Number

The contents of leaf chlorophyll *a*, chlorophyll *b*, proteins, and hexoses as well as 15 mineral nutrient elements in rosette and root material at 32 DAT and the number of leaves at 22 DAT and 32 DAT were quantified. Overall, 277 QTLs were detected for these traits in the three nutrient regimes, comprising 16 major QTLs that explained more than 25% of the trait variance (Fig. 1; Supplemental Fig. S2). Sixty-eight percent

Table II. Predictors for growth-related traits

Selected predictors (ionomic content in the rosette [_{rs}] or in the root [_{rt}], biochemical and developmental traits) for the growth-related traits (rosette weight, RGR, root weight, and root length) and the percentage of trait variance each predictor explains on its own and altogether (total). The prediction was done for each growth-related trait in the C, K-, and P- conditions and for the response of the trait to potassium (Kresp) and phosphate (Presp) reduction.

Predictor	Rosette Weight					RGR					Root Weight					Root Length				
	C	K-	P-	Kresp	Presp	C	K-	P-	Kresp	Presp	C	K-	P-	Kresp	Presp	C	K-	P-	Kresp	Presp
Chlorophyll a																0.7		0.4		
Chlorophyll b	13.0										18.5		4.8		6.5	0.5				
Proteins				7.1						4.3	5.4									
Hexoses																				
B_rs	12.2																		6.0	2.3
B_rt													16.6							
Ca_rs		2.3	1.4				8.0			5.3			5.9							0.4
Ca_rt	3.3			13.1							2.7				7.6	5.5	15.5	3.0		
Cd_rs																				
Cd_rt																				
Co_rs																				
Co_rt																1.3	8.6			
Cu_rs		6.5																		
Cu_rt	2.5						2.4						0.0						4.8	5.7
Fe_rs			18.9	5.7															0.8	
Fe_rt		25.1		12.1		10.9	8.9	6.0		1.7		20.7		6.6	0.7	0.2				6.2
K_rs	38.2	39.1	21.9	7.6	0.8	14.1				0.0		17.5	13.6				0.1			3.4
K_rt		3.5	14.4		3.0			11.2			16.8		15.6		4.6	6.4				
Mg_rs							2.6						0.0							
Mg_rt														4.6	1.7	1.7	1.3	1.3		
Mn_rs				0.1																
Mn_rt					13.7										2.7					24.8
Mo_rs				0.6			0.8			0.6										1.4
Mo_rt		7.7	3.6	2.1		6.7						5.9	0.8	6.7		4.7				2.0
Na_rs		12.1									1.9		6.0							
Na_rt			0.1						3.4						0.9					
Ni_rs	0.1																			
Ni_rt																				
P_rs	2.2	1.8	20.7		1.3		2.0	16.1					17.2							11.9
P_rt	19.8	17.1	6.0	7.5	0.8		6.8	0.5				10.7	1.5							7.4
Rb_rs											10.3		13.0							0.0
Rb_rt													0.3							
S_rs		5.3			7.2							5.8	10.9	14.0	5.8	6.4		11.7		
S_rt	13.5			0.4	0.9							3.8								11.0
Zn_rs								0.1					11.7			5.4		4.1		
Zn_rt	4.3	8.7	20.1	1.4		9.3		27.0				11.7	15.3	33.6		4.3	16.7			
L22	8.1		4.4	15.9	10.4				3.4			1.2		1.2	6.7					0.2
L32	1.3								0.5			1.0	0.4	3.9						0.7
Total	82.3	84.7	83.9	64.4	48.1	40.8	42.0	55.3	3.4	23.5	66.2	73.9	78.2	28.4	18.9	47.7	47.4	54.1	28.0	46.7

of these QTLs had an effect significantly different between the nutrient regimes tested ($G \times E$). In addition, 33 and 12 response QTLs were detected for the reduced potassium and phosphate supplies, respectively. One of these response QTLs explained over 25% of the variation observed in molybdenum content in the rosette in response to the lowered phosphate supply. QTLs for some traits were observed in all conditions, although their effect was condition dependent. This is the case for QTLs for molybdenum content (Mo_rs and Mo_rt in bin 2-4; Fig. 1A), for phosphate and for magnesium content (P_rs and Mg_rt in bin 3-1), for sodium content (Na_rs in bin 4-2/4-3), and for potassium and rubidium content (K_rs and Rb_rs in bin 5-5/5-6).

Colocalization of QTLs for Growth-Related Traits and Predictors

Because variation of growth-related traits has been partially and significantly explained by the variation of chlorophyll, protein, hexose, ionomic traits. or leaf number, we investigated colocalization between QTLs of growth-related traits and predictors to reveal common genetic bases between them. These colocalizations of QTLs for predictors were on average 11.5% more frequent than for nonpredictors, and this difference was highly significant (χ^2 test; $P < 0.0005$) for each growth-related trait and condition. In fact, QTLs of root weight and root length on top of chromosome 1 were present in all nutrient regimes and colocalized

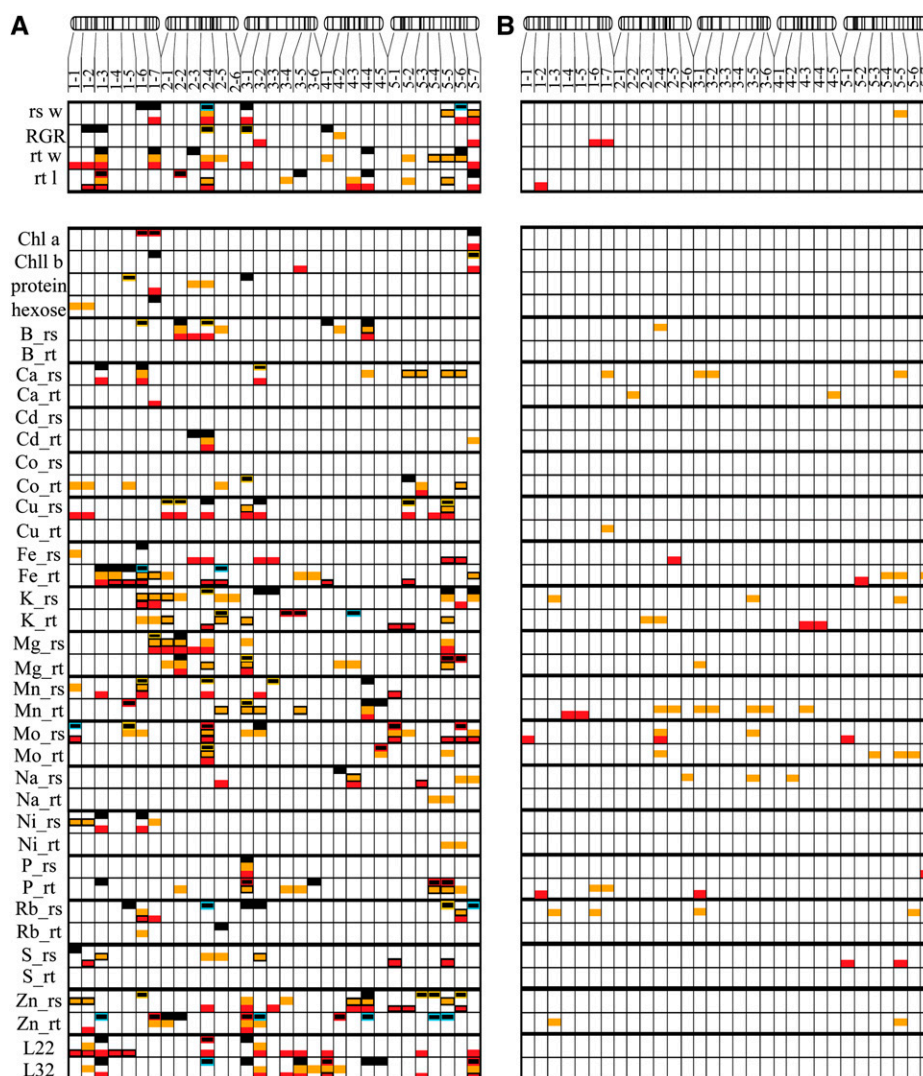


Figure 1. QTL mapping for growth-related traits (rosette weight [rs w], RGR, root weight [rt w], and root length [rt l]), for chlorophyll (Chl a, Chl b), protein, hexose, and ionic traits, and for leaf number (at day 22 [L22] and day 32 [L32]). The five chromosomes of *Arabidopsis* are presented above each panel (chromosomes 1 to 5 from left to right). The genetic positions of the markers that were used to elaborate the genetic map are reported by vertical bars on each chromosome. The ionic traits are represented by their element abbreviations, and the examined tissues are the rosette (_rs) and the root (_rt). The chromosomes were divided into bins of 15 cM (for more detailed characterization of these QTLs, see Supplemental Table S1). A, QTL detection for the traits quantified in the C (black boxes), K⁻ (orange boxes), and P⁻ (red boxes) hydroponic solutions. For each trait, the QTL models obtained in each condition were tested in the other conditions, and significant QTL \times E interactions are shown (see “Materials and Methods”). For the QTLs detected in the control condition, orange and red rims around the QTL boxes indicate that a significantly different effect was detected between C and K⁻ and between C and P⁻ conditions, respectively. QTLs reported with blue rims indicate that a significantly different effect of this QTL was found between C and both K⁻ and P⁻ conditions. For the QTLs detected in the K⁻ or P⁻ conditions, black rims indicate a significantly different effect of this QTL when compared with the control condition. B, QTL detection for trait responses to the K⁻ (orange) and P⁻ (red) regimes.

with several predictor QTLs (bin 1-3; Fig. 1A). Among them were QTLs for root iron content (Fe_{rt}) that were present in all conditions. Another growth QTL for the response of root length to P⁻ was located close to this position (bin 1-2) and colocalized with the root phosphate content QTL for the response to the P⁻ regime. Close to the *Erecta* marker on chromosome 2, major QTLs of molybdenum content were detected (bin 2-4).

Several growth-related trait QTLs were detected at the *Erecta* locus that explained a high variation of rosette weight and root weight in all nutrient regimes. On the top of chromosome 3, QTLs for phosphate content were detected in almost all conditions (bin 3-1). This hotspot of phosphate content QTLs coincided with QTLs for rosette weight, RGR, and root weight, which were only present in the control and/or P⁻ regime.

The only response QTL in the K⁻ regime (bin 5-5) colocalized with response QTLs for the rosette potassium content (K_{rs}), which is a predictor of the rosette weight response to K⁻ (Table II). Furthermore, not only the response of rosette potassium content is a predictor for rosette weight response, but the rosette potassium content in all single conditions (C, K⁻, P⁻) is also a predictor for rosette weight. In accordance with this, we detected in this bin (bin 5-5/5-6) QTLs for rosette weight and QTLs for rosette potassium content (in all conditions). However, large effect QTLs for nonpredictor traits colocalized with growth-related traits (Fig. 1A; Supplemental Fig. S2). This is the case for QTLs for rosette sodium content, which were detected in all conditions (bin 4-2/4-3) and colocalized with root length QTLs (bin 4-3/4-4), even though rosette sodium content is not a predictor for root length.

Validation of the Rosette Weight Response QTL to the K⁻ Regime and Accompanying Ion Changes

Some of the detected QTLs described above colocalized with previously cloned QTLs for similar traits (Alonso-Blanco et al., 2009; see "Discussion"), and it is most probable that the previously cloned genes are also the ones underlying the effects of the QTLs in this study (see "Discussion"). However, the QTL for rosette weight response on the bottom of chromosome 5 has not been described before. Although QTLs for rosette weight have been detected at this locus in all the nutrient regimes tested, its effect is significantly different in the K⁻ regime than in the other conditions (Fig. 1; Supplemental Fig. S2; Supplemental Table S1). In accordance, a response QTL for rosette weight has been detected at this locus (bin 5-5). To validate the presence of this QTL, three NILs carrying the alleles of Kas-2 at the bottom of chromosome 5 in an otherwise *Ler* background were selected (Fig. 2A), and responses of rosette weight to lowered potassium supply were quantified and compared with the response of *Ler* (Fig. 2B). Whereas the rosette weight was decreased by 34.3% in *Ler* grown in the reduced potassium medium compared with the control, the rosette weight of the three selected NILs was much less affected (10.7%–15.3%). These significant differences between the NILs and *Ler* confirmed the presence of the detected rosette weight response QTL on the bottom of chromosome 5.

In addition, we investigated the alterations in ion content due to the presence of Kas-2 alleles at this locus. In the control and the reduced potassium conditions, 29 ionic QTLs have been detected on the bottom of chromosome 5 (Supplemental Table S1). Validations of these QTLs were also performed by comparing the ion content of *Ler* and one selected NIL (NIL3; Fig. 3). The QTLs for potassium content in the rosette (predictor for rosette weight) detected in both the control and the reduced potassium regimes have been validated, and as expected, the Kas-2 alleles increased the potassium content in NIL3. Nine other

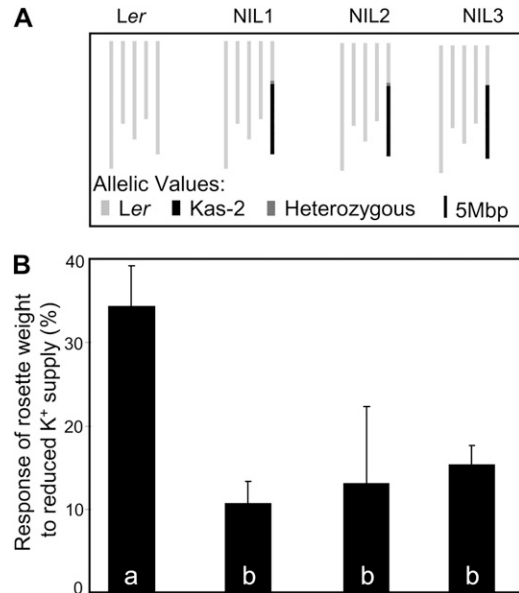


Figure 2. Validation of the rosette weight response QTL for the K⁻ regime. A, Graphic representation of the genotypes of *Ler* and the selected NILs carrying an introgression of Kas-2 alleles on the bottom of chromosome 5 (for detailed genotyping, see Supplemental Fig. S3). B, Response of rosette weight to lowered potassium supply for the lines represented in A (mean \pm SE; $n = 3$ experiments). Values with differing letters are significantly different at $P < 0.05$.

ion content QTLs have been validated using NIL3 (in C, P_{rt}, Rb_{rs} (twice); and in K⁻, Co_{rt}, Cu_{rs}, Na_{rs}, P_{rt}, Rb_{rs}, Zn_{rs}; Fig. 3). One QTL has been validated but with an opposite allelic effect (magnesium content in the rosette for the K⁻ regime; Fig. 3B). In contrast, 14 QTLs were not validated using this approach. Nonetheless, although the differences between NIL3 and *Ler* were not significant for these ion contents, the observed tendencies in ion content differences between *Ler* and NIL3 were as expected from the QTL analysis in nearly all cases (except in K⁻, Mo_{rt}, Na_{rt}, Ni_{rt}). Furthermore, six other significant differences between the ion content of NIL3 and *Ler* have been revealed that were not expected from the QTL analysis (in C, B_{rt}, Fe_{rs}, Na_{rt}, Ni_{rt}; and in K⁻, Co_{rs}, Mn_{rt}; Fig. 3).

Several QTLs for predictors of rosette weight were validated with *Ler* and NIL3 in the control (K_{rs} and P_{rt}) or in the reduced potassium supply (Cu_{rs}, K_{rs}, Na_{rs}, and P_{rt}) regime, respectively. In the control, these predictors explained between 20% and 38% of the variation of rosette weight, and in K⁻ they explained between 12% and 39% (except for Cu_{rs}, which explained 7%; Table II).

DISCUSSION

A set of *Ler* \times Kas-2 RILs (El-Lithy et al., 2006) was grown hydroponically in three different mineral nu-

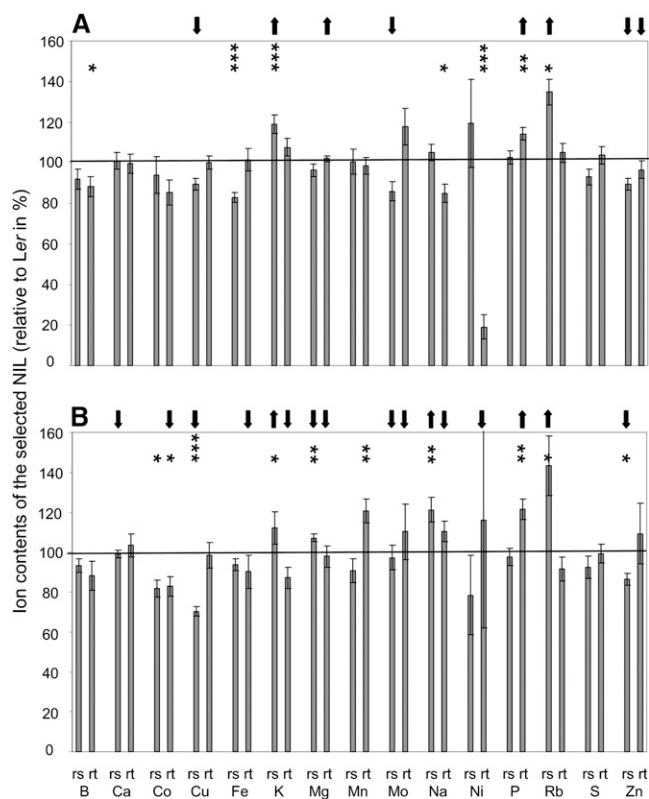


Figure 3. Ion content of a selected NIL. Ion content of NIL3 (Fig. 2A) grown in C medium (A) or in K⁻ medium (B). The ion content in the rosette (_rs) and the root (_rt) is expressed as a percentage change compared with the that of *Ler* (set as 100%). Significant differences between the NIL and *Ler* are indicated (* $P < 0.05$, ** $P < 0.005$, *** $P < 0.001$). The arrows indicate the presence of a detected QTL for the corresponding ion content, and the direction indicates if the Kas-2 alleles have a positive or negative effect on this ion content (up and down arrows, respectively). In some cases, QTLs for the same trait and with the same allelic effect collocated (in C, K_{rs}, Rb_{rs}, Zn_{rs}; in K⁻, K_{rs}); these QTLs are indicated by only one arrow here.

trient regimes: C, K⁻, and P⁻. Growth-related traits (rosette weight, root weight, root length, and RGR) of all the lines were measured in each condition as well as ionic and biochemical traits. Variation among these traits in each condition enabled us to detect a total of 327 QTLs, spread over the entire genome of *Arabidopsis*.

We detected QTLs for each growth-related trait in plants grown in C, K⁻, and P⁻ media. Some of the QTLs detected in our study explained up to 22% of the phenotypic variation. However, most of them explained only a small percentage of this variation. This low number of major growth-related QTLs is in accordance with the idea that variation of complex traits like growth is governed by many small-effect QTLs (Kroymann and Mitchell-Olds, 2005). Nonetheless, we identified 16 major QTLs, which explained between 25% and 62% of the ionic variation. The detection of QTLs showed that the different nutrient

regimes had an impact on the genetic determinism for most of the quantified traits, and a significant G × E interaction effect has been revealed for 60% of the QTLs. This environmental effect was confirmed through the detection of QTLs for the trait responses to environment, with response expressed as change in the percentage of a trait in the reduced nutrient supply compared with the control. Most of these response QTLs collocated with G × E QTLs and explained between 6.1% and 22.1% of phenotypic variation, with the exception of molybdenum content in response to reduced phosphate supply, which explained 40.9%.

In addition, a successful attempt to link growth-related traits and ionic/biochemical/developmental traits was performed across different mineral regimes. Although previous studies have shown a high correlation between several carbohydrates and growth (Meyer et al., 2007; Sulpice et al., 2009), in our study total hexose content of the rosette was not found to be significantly associated with any of the variation of growth-related traits. We found a strong correlation between the variation of growth-related and ionic traits, especially for the root and the rosette weight, for which ionic variation explained between 70% and 85% of the variation, respectively. Correlations between the growth-related traits concurred with the number of common predictors found for these traits, emphasizing the impact of common predictors on growth per se.

Furthermore, QTLs of growth-related traits were found to collocate with QTLs of their predictors, and candidate genes responsible for these traits can be suggested within these genomic regions. For instance, the phosphate response QTL on the top of chromosome 1, which influenced variation in root length in reduced phosphate medium, collocated with a QTL for primary root growth arrest in response to phosphate starvation (Reymond et al., 2006). The QTL for primary root growth arrest has previously been cloned and identified as the gene *LPR1*, a multicopper oxidase that is involved in the perception of low phosphate status in the root cap (Svistonoff et al., 2007). Ward et al. (2008) suggested that the primary root growth arrest could also be due to iron toxicity caused by a greater availability of iron in a reduced phosphate medium, implicating a role of *LPR1* in iron distribution or uptake rather than in phosphate sensing. Interestingly, we detected a QTL for iron content collocating with the root length QTL at the *LPR1* position.

Moreover, we detected QTLs for most growth-related traits as well as molybdenum content at the *Erecta* locus on chromosome 2 in all nutrient regimes. The studied RIL population is derived from a laboratory strain (*Ler*) for which the *Erecta* gene is mutated (Ungerer et al., 2002; Koornneef et al., 2004). This mutation is segregating among the RILs. *Erecta* encodes a receptor-like kinase involved in leaf, stem, and flower development (Torii et al., 1996; van Zanten

et al., 2009). Also, for other populations derived from *Ler*, growth QTLs at this locus have already been reported (Ungerer et al., 2002; El-Lithy et al., 2004; Tisné et al., 2008). Therefore, the *Erecta* gene itself is a good candidate to explain the growth-related trait QTLs detected in all these studies, including ours. Baxter et al. (2008a) showed that variation in molybdenum content across several accessions of *Arabidopsis* is controlled by a putative molybdenum transporter (*MOT1*), which is located close to the locus of *Erecta*. Therefore, the variation of growth and the variation of molybdenum content are correlated, probably due to genetic linkage of *Erecta* and *MOT1*.

The group of QTLs at the top of chromosome 3, containing a major QTL for phosphate content, colocalized with several growth-related traits that were only detected either in the control and/or reduced phosphate regime. QTLs for phytate and phosphate content in seeds and leaves have been previously identified at a similar position on chromosome 3 (Bentsink et al., 2003; using a *Ler* × Cape Verde Islands RIL population), and a vacuolar membrane ATPase subunit was considered to be a likely candidate underlying the effect of this QTL. Studies in the *Ler* × Antwerp-1 RIL population have also identified a phosphate concentration QTL on the top of chromosome 3 (Ghandilyan et al., 2009).

The QTL for sodium content on chromosome 4 colocalized with a sodium transporter gene, *AtHKT1*, which is known to cause sodium content changes between several natural accessions of *Arabidopsis* (Rus et al., 2006). Our study revealed that the sodium QTL colocalized with growth QTLs of root length. This transporter is known to function in the root to control both root and shoot sodium content (Mäser et al., 2002), and variation at this locus, therefore, could be implicated in the length variation we observed. However, sodium rosette content does not predict root length, and this colocalization could be due to the linkage of different genes.

Although some QTLs detected in our study colocalized with already known and cloned QTLs in *Arabidopsis*, most of them, to our knowledge, have never been reported. This is the case for the rosette weight response QTLs located on the bottom of chromosome 5, for which also a significant QTL × E interaction has been detected. In addition, this QTL is the only significant growth-related QTL in response to the K⁻ regime. As a response QTL, it may be involved in the adaptation of the plant to reduced potassium availability. Because this QTL was of rather low effect ($R^2 = 9.3\%$), it was necessary to validate its effect by selecting suitable NILs (Alonso-Blanco and Koornneef, 2000; Reymond et al., 2007). The phenotypes of the NILs clearly validated the presence of the detected QTL for the response of rosette weight to the reduced potassium regime. We found that the NILs retained more than 20% fresh weight in the reduced potassium supply than *Ler*, and the Kas-2 allele on the bottom of chromosome 5 conferred a growth advantage to the plants under these conditions.

This QTL colocalized with 29 ion content QTLs, among them QTLs for potassium content for plants grown in both the control and the reduced potassium regimes. Ion contents of NIL3 have been quantified in order to confirm this result. The ion content QTLs were generally of low effect. Low-effect QTLs are difficult to validate due to the complex genetics of those traits (Kroymann and Mitchell-Olds, 2005); therefore, it is not surprising that several ion content QTLs could not be validated, but only insignificant tendencies in ion content differences were observed between the lines. However, NIL3 showed a significantly higher potassium content in the rosette compared with *Ler*. Additionally, the rubidium content was also significantly higher in the NIL than in *Ler* (Fig. 3). Rubidium is a well-established chemical analog of potassium, and plant physiologists have used radioactive ⁸⁶Rb for a long time to measure potassium uptake (Läuchli and Epstein, 1970; Pyo et al., 2010). Thus, rubidium quantification offers an independent replication of the potassium quantification. Subsequently, QTLs for rosette potassium and rubidium content colocalized on the bottom of chromosome 5 (Fig. 1), and elevated potassium and rubidium contents quantified in NIL3 validated these QTLs. The fact that the NIL had higher potassium content than *Ler* might contribute to its growth advantage in the reduced potassium supply condition.

Additionally, it is worth noting that major predictors for rosette weight in both control and K⁻ regimes have been detected on the bottom of chromosome 5. Quantification of those predictors in NIL3 and *Ler*, which showed different growth patterns, not only enabled us to validate these QTLs but also support our choice of predictors (Table II), as variation in predictors went along with differential growth effects between the lines.

CONCLUSION

Overall, we were able to explain up to 85% of phenotypic variation in growth primarily with ionic predictors. Our study highlights the importance of broader phenotypic quantification, with a particular focus on ionic traits as being important drivers of growth. One of the detected growth-response QTLs was validated with NILs that retained over 20% more rosette weight in reduced potassium supply. This growth advantage was in accordance with a significant change in ionic predictors that explain a high percentage of the variation in rosette weight. Further studies focusing on the identification of both molecular mechanisms underlying the relationship between the ionome and plant growth will provide new insights into the cellular biochemistry of growth.

MATERIALS AND METHODS

Plant Material

A total of 125 *Arabidopsis* (*Arabidopsis thaliana*) RILs derived from a cross between *Ler* (from Poland) and Kas-2 (from Kashmir; El-Lithy et al., 2006)

were used for the QTL detection. Eighty-nine polymorphic markers were used to genotype all the RILs and to build a genetic map (JoinMap4; Kyazama). The length of the genetic map was 431.17 cM, and the average distance between markers was 4.84 cM (the maximum distance between markers being 13.88 cM, between *snp204* and *snp97* on chromosome 5). Three NILs were selected among the F2 population obtained from a back-cross between *Ler* and RIL 138. For the genotypic characterization of the NILs (Supplemental Fig. S3), new simple sequence length polymorphism and cleaved amplified polymorphic sequence markers were designed (Supplemental Table S2) based on polymorphism information from the Multiple SNP Query Tool (<http://msq.weigeltworld.org>).

Growth Conditions

Plants were sown on top of agar (0.65% *Daishin* agar; Duchefa Biochemie)-filled 0.5-mL microtubes with the tip removed. The tubes were soaked in nutrient solution containing one of the following: (1) Control (C), KNO₃ 2,000 μM, CaCl₂·2H₂O 300 μM, MgSO₄·7H₂O 150 μM, KH₂PO₄ 150 μM, H₃BO₃ 10 μM, MnSO₄·H₂O 15 μM, ZnSO₄·7H₂O 3 μM, KI 0.5 μM, Na₂MoO₄·2H₂O 0.1 μM, CuSO₄·5H₂O 0.01 μM, CoCl₂·6H₂O 0.01 μM, FeSO₄·7H₂O 22.4 μM, Na₂EDTA 22.3 μM, Ca(NO₃)₂·4H₂O 1,000 μM; (2) reduced potassium supply (K⁻), KNO₃ 0 μM, CaCl₂·2H₂O 300 μM, MgSO₄·7H₂O 150 μM, KH₂PO₄ 150 μM, H₃BO₃ 10 μM, MnSO₄·H₂O 15 μM, ZnSO₄·7H₂O 3 μM, KI 0.5 μM, Na₂MoO₄·2H₂O 0.1 μM, CuSO₄·5H₂O 0.01 μM, CoCl₂·6H₂O 0.01 μM, FeSO₄·7H₂O 22.4 μM, Na₂EDTA 22.3 μM, Ca(NO₃)₂·4H₂O 2,000 μM; or (3) reduced phosphate supply (P⁻), KNO₃ 2,000 μM, CaCl₂·2H₂O 300 μM, MgSO₄·7H₂O 150 μM, KH₂PO₄ 32 μM, H₃BO₃ 10 μM, MnSO₄·H₂O 15 μM, ZnSO₄·7H₂O 3 μM, KI 0.5 μM, Na₂MoO₄·2H₂O 0.1 μM, CuSO₄·5H₂O 0.01 μM, CoCl₂·6H₂O 0.01 μM, FeSO₄·7H₂O 22.4 μM, Na₂EDTA 22.3 μM, KCl 118 μM, Ca(NO₃)₂·4H₂O 1,000 μM.

The solutions were buffered with 2.39 mM MES (adjusted to a pH of 6.00 with KOH). The final pH of the solutions was 5.80. After a 4-d cold treatment, the tubes containing the plants were transferred to a climate-controlled cabinet (AR95L; Percival Scientific). The plants were grown in an 81-hole tray suspended in nutrient solution (Tocquin et al., 2003). They were kept in 8 h of light and 16 h of dark with an average intensity of 15,000 lux (with additional 15 min of light provided by bulbs of 200 lux before and after the onset of the light), with a temperature of 22°C and a humidity of approximately 60% during the light period and a temperature of 18°C and a humidity of approximately 80% during the dark period. For the mapping experiments, nine replicates were grown for each RIL.

For the validation of the potassium response QTL, the same growth conditions mentioned above have been applied but with a lower potassium supply for the K⁻ nutrient regime: KNO₃ 0 μM, KH₂PO₄ 107 μM, Ca(NO₃)₂·4H₂O 2,000 μM, Ca(H₂PO₄)₂·H₂O 21.5 μM (the other ion concentrations did not vary from the control solution). The solution was buffered with 2.39 mM MES (adjusted to a pH of 6.00 with NaOH), and the plants were grown in a randomized sowing scheme with five, 10, or 11 replicates depending on the experiment.

Quantification of the Traits

Photographs of the trays were taken at 7, 10, 15, 17, 20, and 22 DAT from the 4°C stratification treatment into the light, and projected leaf area (cm²) for each plant, and for each date, was quantified using Image Pro Analyzer 6.0 (Mediacybernetics). The RGR was calculated based on the projected leaf area and represents the slope of the exponential change in projected leaf area over time. The leaf number was scored at 22 and 32 DAT. Plants were harvested at 32 DAT, and the fresh weight of the rosette and the roots as well as root length (complete length of the root apparatus stretched out on a straight surface) of each plant were quantified. The response of a trait was calculated as the percentage change of the trait observed in plants grown in the nutrient solution with lowered mineral nutrient supply compared with plants grown in the control solution: $((\text{trait}_{\text{in control}} - \text{trait}_{\text{in K}^-/\text{P}^-}) / \text{trait}_{\text{in control}}) \times 100$.

In addition, the leaves were also analyzed for hexose, protein, and chlorophyll contents. Approximately 300 to 500 mg of fresh leaf material was ground, and the cell debris was washed three times with 500 μL of 80% ethanol and heated at 80°C for 10 min to extract sugars and chlorophylls. Half of the extraction (750 μL) was kept on ice in opaque 2-mL microtubes (Sigma-Aldrich) followed by the colorimetric analysis at three different wavelengths (646, 663, and 750 nm). The levels of chlorophyll *a* (Chla) and *b* (Chlb) were calculated as followed:

$$\text{Chla} = (12.5 \times (\text{OD}_{663} - \text{OD}_{750}) - 2.55 \times (\text{OD}_{646} - \text{OD}_{750}))$$

$$\text{Chlb} = (20.5 \times (\text{OD}_{646} - \text{OD}_{750}) - 4.91 \times (\text{OD}_{663} - \text{OD}_{750}))$$

where OD represents optical density.

The amount of chlorophyll was divided by the quantity of used fresh weight and the volume of extract used for the colorimetric analysis. The other half of the sample (750 μL) was dried overnight in a rotary evaporator. The pellet was dissolved in 500 μL of deionized water, and the quantification of total hexoses was performed according to Viola and Davies (1992). Protein extraction was performed by washing cell debris of 300 to 500 mg of crushed, fresh leaf material three times with 300 μL of 0.1 M Tris-HCl/0.1% Triton X-100, pH 7, by vortexing it for 10 min. Protein quantification was done on 96-well microtiter plates using Coomassie Plus Protein Assay Reagent (Thermo Scientific).

For the analysis of mineral nutrients in plant tissues, approximately 2 to 8 mg of dried powdered lyophilized tissue was placed into 100- × 16-mm Pyrex tubes and digested with 0.7 mL of concentrated HNO₃ (Mallinckrodt; AR Select grade) at 110°C for 4 h. Each sample was diluted to 6.0 mL with 18 M water and analyzed on a Perkin-Elmer Elan DRce inductively coupled plasma mass spectrometry. Indium (EM Science) was used as an internal standard. National Institute of Standards and Technology traceable calibration standards (ULTRAScientific) were used for the calibration. For each genotype, three samples containing pooled plant material of three individual plants were used for the QTL detection. Plant material from four experiments was used for obtaining rosette material for the ionic quantification of NIL3 and *Ler*, whereas plant material from two experiments was used for obtaining root material. Three samples per genotype and condition were quantified, with each sample containing on average the root material of three individual plants or the rosette material of four individual plants.

Statistical Analyses

Phenotypic Data Analysis

For each trait in each of the three treatments (C, K⁻, P⁻), adjusted entry means were calculated for all RILs based on the model

$$y_{ij} = \mu + \text{RIL}_i + e_{ij}$$

where y_{ij} is the phenotypic observation of the *i*th RIL in the *j*th block, μ is the general mean, RIL_i is the effect of the *i*th RIL (regarded as fixed), and e_{ij} is the residual. Furthermore, heritability on an entry mean basis was calculated, where σ_g^2 was the genotypic variance and \bar{w} was the mean phenotypic variance of the difference between two adjusted entry means (Holland et al., 2003), based on the following formula:

$$h^2 = \frac{\sigma_g^2}{\sigma_g^2 + \bar{w}/2}$$

For each of the growth-related traits (rosette weight, root weight, root length, and RGR), we performed separately all subset multiple regressions based on the Schwarz (1978) Bayesian criterion to select those traits from the following list that best explain the variation: B_rs, B_rt, Ca_rs, Ca_rt, Cd_rs, Cd_rt, Co_rs, Co_rt, Cu_rs, Cu_rt, Fe_rs, Fe_rt, K_rs, K_rt, Mg_rs, Mg_rt, Mn_rs, Mn_rt, Mo_rs, Mo_rt, Na_rs, Na_rt, Ni_rs, Ni_rt, P_rs, P_rt, Rb_rs, Rb_rt, S_rs, S_rt, Zn_rs, Zn_rt (with "rs" being the respective ion content in the rosette and "rt" in the roots), chlorophyll *a* and *b*, total leaf proteins, total leaf hexoses, leaf number at 22 DAT (L22), and leaf number at 32 DAT (L32). These calculations were performed using R package leaps. Furthermore, we used multivariate all subset multiple regression in order to identify the traits best explaining the variation of all growth-related traits together. The traits selected are called "predictors." To test whether the occurrence of colocalization for growth-related trait QTLs and their predictor QTLs is higher than for the nonpredictor QTLs, a χ^2 test was performed. The test compared the frequency of the colocalizing and the noncolocalizing QTLs for predictors and nonpredictors for each growth-related trait in each condition.

QTL Analyses

For each trait, the values per RIL were averaged, and a QTL analysis was performed with MapQTL 5.0 (Van Ooijen, 2004; Kyazama) using the Multiple

QTL Models procedure. This approach consists first of selecting cofactors, which are markers selected to take over the role of nearby putative QTLs. Markers used as cofactors have been chosen by backward selection, and for each QTL detected, a marker near the QTL has been used as a cofactor in the final model (Supplemental Table S1). With this Multiple QTL Models mapping, a one-dimensional search over the genome is performed by testing for segregating QTLs as in interval mapping while simultaneously fitting the selected cofactors (Jansen and Stam, 1994). Incompatible lines (Alcázar et al., 2009) were removed from the QTL analysis in order to avoid confusion of effects on growth-related traits. A permutation test using 1,000 permutations of the original data resulted in a genome-wide 95% logarithm of the odds (LOD) threshold of 2.4 on average over all the traits (2.417 ± 0.137). The length of the QTL was determined according to a LOD - 1 support interval. Analysis of QTL \times E interactions has been performed using the statement E in PLABQTL version 1.2 (H.F. Utz and A.E. Melchinger, unpublished data) on the set of previously detected QTLs.

For comparison of the selected NILs with the *Ler* parental line, the SE between the responses of three independent experiments was calculated and the statistical significance was tested with a Student-Newman-Keuls test.

For the ionic comparison between NIL3 and *Ler*, the significance was tested with an ANOVA (univariate linear model; using SPSS 13.0 for Windows).

Supplemental Data

The following materials are available in the online version of this article.

Supplemental Figure S1. Correlations of the selected predictors for the growth-related traits.

Supplemental Figure S2. QTL mapping for growth-related traits (rosette weight, RGR, root weight, and root length), for chlorophyll (Chla, Chlb), protein, hexose, and ionic traits (for rosette [rs] and root [rt] tissue), and for leaf number at 22 DAT (L22) and 32 DAT (L32).

Supplemental Figure S3. Graphic presentation of the genotypes of *Ler*, RIL138, and the NILs.

Supplemental Table S1. List of all detected QTLs.

Supplemental Table S2. Primers designed for genotyping of the NILs.

ACKNOWLEDGMENTS

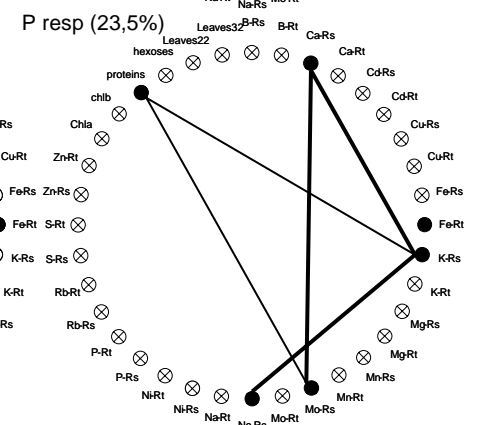
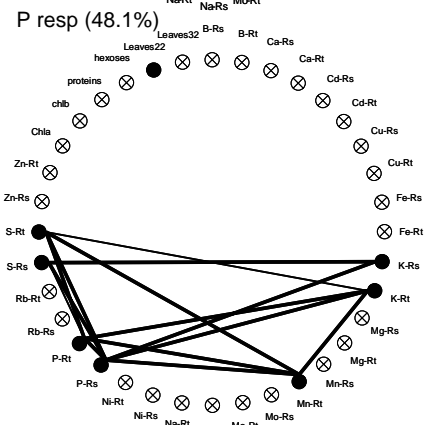
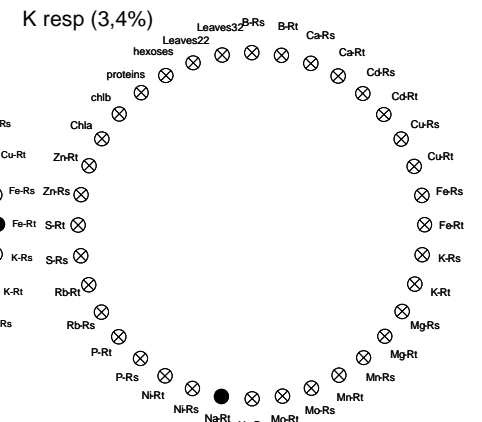
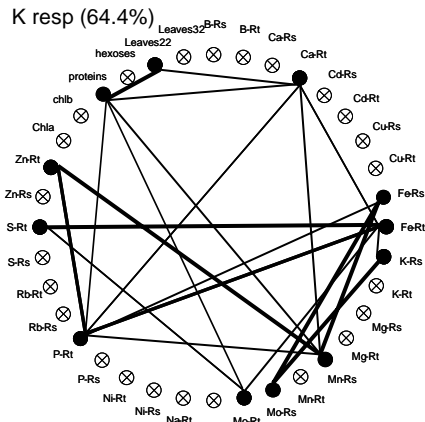
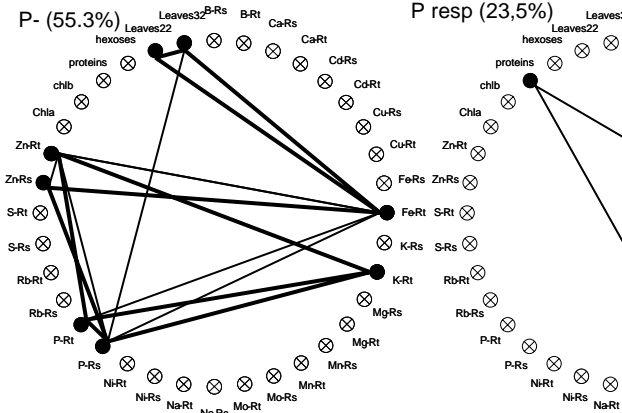
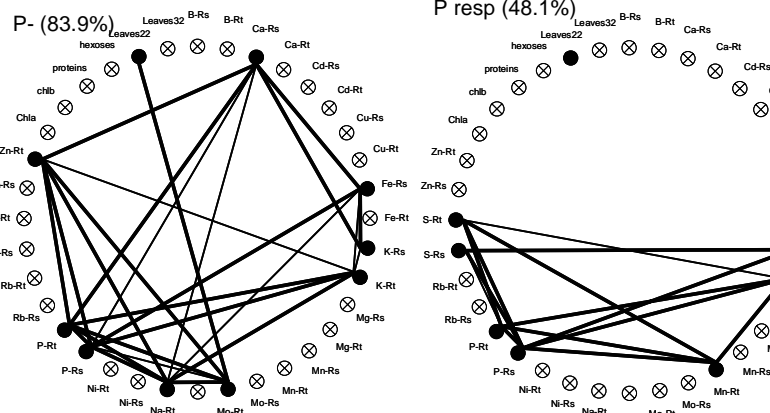
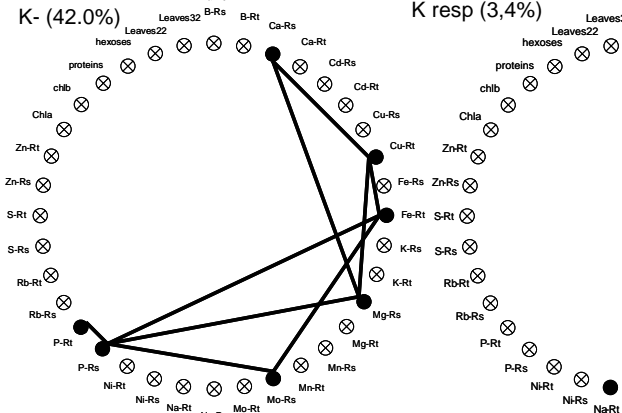
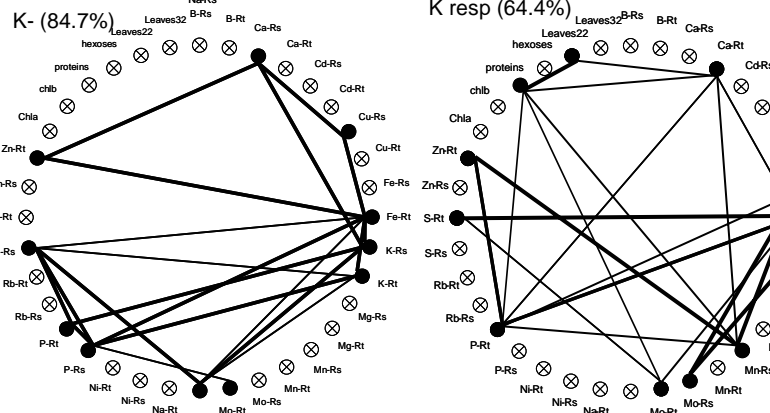
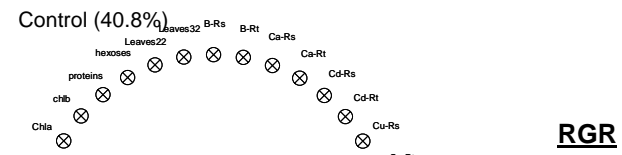
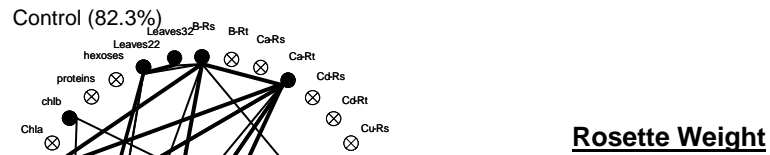
We are grateful to Maarten Koornneef for critical comments. We also thank Barbara Eilts for her meticulous technical support and Regina Gentges for highly valued help in the greenhouse. We acknowledge Bjorn Pieper for sharing F1 seeds from the cross between RIL138 and *Ler*. We also thank Alexis Walker for grammatical and spelling corrections to the manuscript.

Received June 16, 2010; accepted September 5, 2010; published September 8, 2010.

LITERATURE CITED

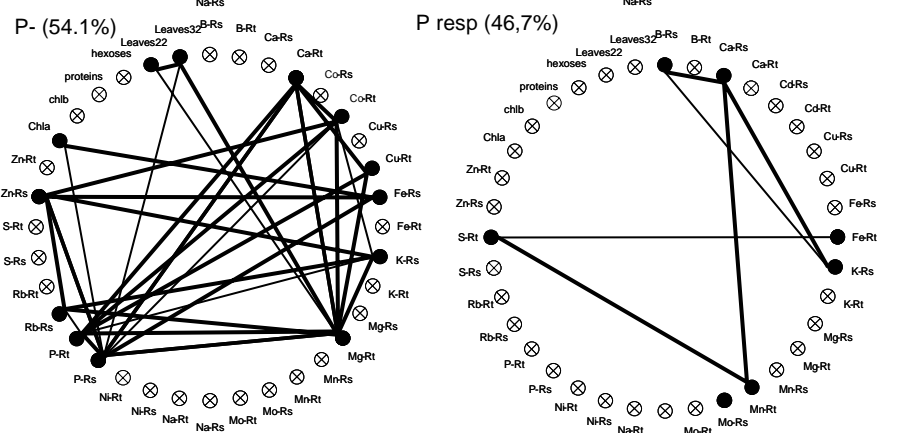
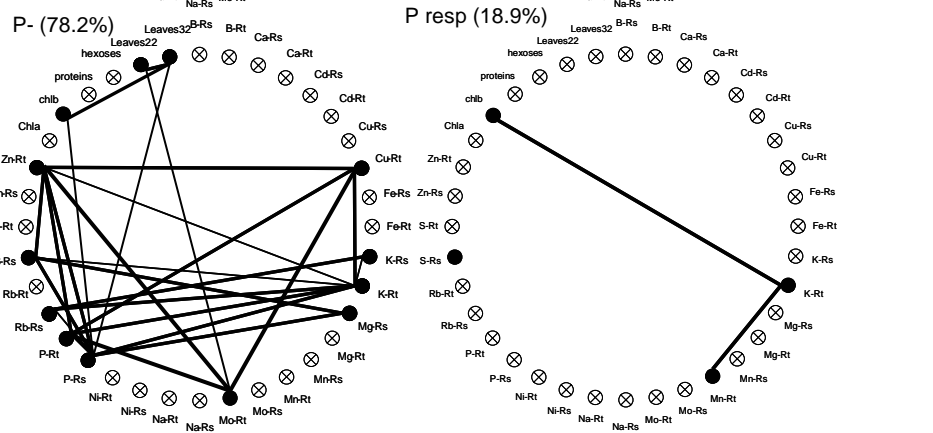
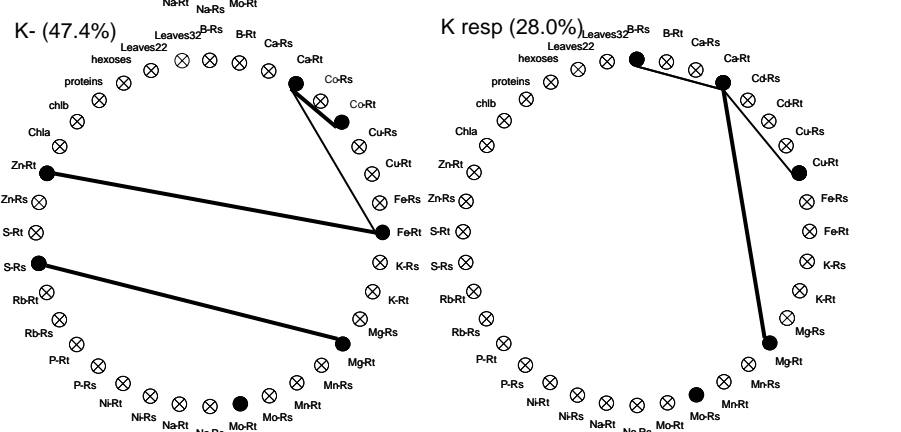
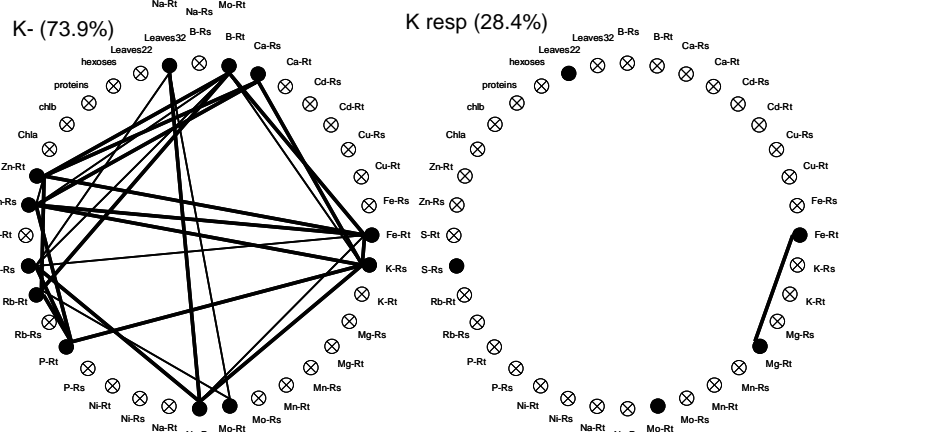
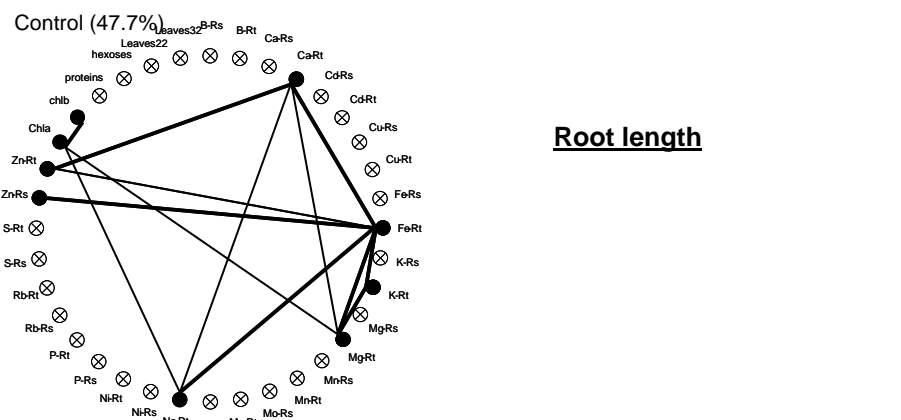
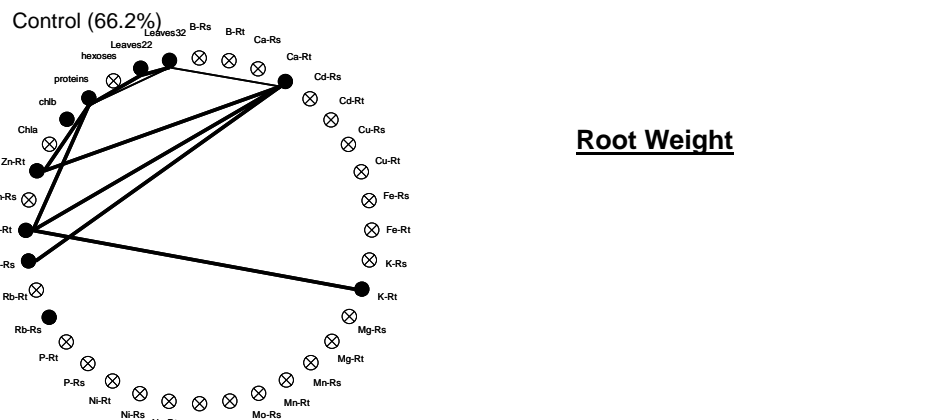
- Abel S, Ticconi CA, Delatorre CA (2002) Phosphate sensing in higher plants. *Physiol Plant* **115**: 1–8
- Alcázar R, García AV, Parker JE, Reymond M (2009) Incremental steps toward incompatibility revealed by *Arabidopsis* epistatic interactions modulating salicylic acid pathway activation. *Proc Natl Acad Sci USA* **106**: 334–339
- Alonso-Blanco C, Aarts MG, Bentsink L, Keurentjes JJ, Reymond M, Vreugdenhil D, Koornneef M (2009) What has natural variation taught us about plant development, physiology, and adaptation? *Plant Cell* **21**: 1877–1896
- Alonso-Blanco C, Koornneef M (2000) Naturally occurring variation in *Arabidopsis*: an underexploited resource for plant genetics. *Trends Plant Sci* **5**: 22–29
- Amtmann A, Troufflard S, Armengaud P (2008) The effect of potassium nutrition on pest and disease resistance in plants. *Physiol Plant* **133**: 682–691
- Armengaud P, Breitling R, Amtmann A (2004) The potassium-dependent transcriptome of *Arabidopsis* reveals a prominent role of jasmonic acid in nutrient signaling. *Plant Physiol* **136**: 2556–2576
- Ashley MK, Grant M, Grabov A (2006) Plant responses to potassium deficiencies: a role for potassium transport proteins. *J Exp Bot* **57**: 425–436
- Barto EK, Cipollini D (2005) Testing the optimal defense theory and the growth-differentiation balance hypothesis in *Arabidopsis thaliana*. *Oecologia* **146**: 169–178
- Baxter I, Muthukumar B, Park HC, Buchner P, Lahner B, Danku J, Zhao K, Lee J, Hawkesford MJ, Guerinot ML, et al (2008a) Variation in molybdenum content across broadly distributed populations of *Arabidopsis thaliana* is controlled by a mitochondrial molybdenum transporter (*MOT1*). *PLoS Genet* **4**: e1000004
- Baxter IR, Vitek O, Lahner B, Muthukumar B, Borghi M, Morrissey J, Guerinot ML, Salt DE (2008b) The leaf ionome as a multivariable system to detect a plant's physiological status. *Proc Natl Acad Sci USA* **105**: 12081–12086
- Bentsink L, Yuan K, Koornneef M, Vreugdenhil D (2003) The genetics of phytate and phosphate accumulation in seeds and leaves of *Arabidopsis thaliana*, using natural variation. *Theor Appl Genet* **106**: 1234–1243
- Buchanan BB, Gruissem W, Jones RJ (2002) *Biochemistry and Molecular Biology of Plants*. John Wiley & Sons, West Sussex, UK
- Carroll A, Somerville C (2009) Cellulosic biofuels. *Annu Rev Plant Biol* **60**: 165–182
- Christian M, Steffens B, Schenck D, Burmester S, Böttger M, Lüthen H (2006) How does auxin enhance cell elongation? Roles of auxin-binding proteins and potassium channels in growth control. *Plant Biol (Stuttg)* **8**: 346–352
- Clarkson DT (1980) The mineral nutrition of higher plants. *Annu Rev Plant Physiol* **31**: 239–298
- Di Cera E (2006) A structural perspective on enzymes activated by monovalent cations. *J Biol Chem* **281**: 1305–1308
- Doerner P (2008) Phosphate starvation signaling: a threesome controls systemic P(i) homeostasis. *Curr Opin Plant Biol* **11**: 536–540
- Donohue K, Dorn L, Griffith C, Kim E, Aguilera A, Polisetty CR, Schmitt J (2005) Environmental and genetic influences on the germination of *Arabidopsis thaliana* in the field. *Evolution* **59**: 740–757
- El-Lithy ME, Bentsink L, Hanhart CJ, Ruys GJ, Rovito D, Broekhof JLM, van der Poel HJA, van Eijk MJT, Vreugdenhil D, Koornneef M (2006) New *Arabidopsis* recombinant inbred line populations genotyped using SNPWave and their use for mapping flowering-time quantitative trait loci. *Genetics* **172**: 1867–1876
- El-Lithy ME, Clercx EJM, Ruys GJ, Koornneef M, Vreugdenhil D (2004) Quantitative trait locus analysis of growth-related traits in a new *Arabidopsis* recombinant inbred population. *Plant Physiol* **135**: 444–458
- Elumalai RP, Nagpal P, Reed JW (2002) A mutation in the *Arabidopsis* *KT2/KUP2* potassium transporter gene affects shoot cell expansion. *Plant Cell* **14**: 119–131
- Ghandilyan A, Barboza L, Tisné S, Granier C, Reymond M, Koornneef M, Schat H, Aarts MG (2009) Genetic analysis identifies quantitative trait loci controlling rosette mineral concentrations in *Arabidopsis thaliana* under drought. *New Phytol* **184**: 180–192
- Gilbert N (2009) Environment: the disappearing nutrient. *Nature* **461**: 716–718
- Harada H, Leigh RA (2006) Genetic mapping of natural variation in potassium concentrations in shoots of *Arabidopsis thaliana*. *J Exp Bot* **57**: 953–960
- Holland J, Nyquist W, Cervantes-Martinez C (2003) Estimating and interpreting heritability for plant breeding: an update. *Plant Breed Rev* **22**: 9–112
- Jansen RC, Stam P (1994) High resolution of quantitative traits into multiple loci via interval mapping. *Genetics* **136**: 1447–1455
- Jiang C, Gao X, Liao L, Harberd NP, Fu X (2007) Phosphate starvation root architecture and anthocyanin accumulation responses are modulated by the gibberellin-DELLA signaling pathway in *Arabidopsis*. *Plant Physiol* **145**: 1460–1470
- Jordan-Meille L, Pellerin S (2008) Shoot and root growth of hydroponic maize (*Zea mays* L.) as influenced by K deficiency. *Plant Soil* **304**: 157–168
- Jung JY, Shin R, Schachtman DP (2009) Ethylene mediates response and tolerance to potassium deprivation in *Arabidopsis*. *Plant Cell* **21**: 607–621
- Koornneef M, Alonso-Blanco C, Vreugdenhil D (2004) Naturally occurring genetic variation in *Arabidopsis thaliana*. *Annu Rev Plant Biol* **55**: 141–172

- Korves TM, Schmid KJ, Caicedo AL, Mays C, Stinchcombe JR, Purugganan MD, Schmitt J (2007) Fitness effects associated with the major flowering time gene *FRIGIDA* in *Arabidopsis thaliana* in the field. *Am Nat* **169**: E141–E157
- Kroymann J, Mitchell-Olds T (2005) Epistasis and balanced polymorphism influencing complex trait variation. *Nature* **435**: 95–98
- Lai F, Thacker J, Li Y, Doerner P (2007) Cell division activity determines the magnitude of phosphate starvation responses in *Arabidopsis*. *Plant J* **50**: 545–556
- Läuchli A, Epstein E (1970) Transport of potassium and rubidium in plant roots: the significance of calcium. *Plant Physiol* **45**: 639–641
- López-Bucio J, Hernández-Abreu E, Sánchez-Calderón L, Pérez-Torres A, Rampey RA, Bartel B, Herrera-Estrella L (2005) An auxin transport independent pathway is involved in phosphate stress-induced root architectural alterations in *Arabidopsis*: identification of BIG as a mediator of auxin in pericycle cell activation. *Plant Physiol* **137**: 681–691
- Loudet O, Chaillou S, Merigout P, Talbotec J, Daniel-Vedele F (2003) Quantitative trait loci analysis of nitrogen use efficiency in *Arabidopsis*. *Plant Physiol* **131**: 345–358
- Luan S, Lan W, Chul Lee S (2009) Potassium nutrition, sodium toxicity, and calcium signaling: connections through the CBL-CIPK network. *Curr Opin Plant Biol* **12**: 339–346
- Maathuis FJM, Sanders D (1996) Mechanisms of potassium absorption by higher plant roots. *Physiol Plant* **96**: 158–168
- Marschner H (1995) Mineral Nutrition of Higher Plants, Ed 2. Academic Press, London
- Mäser P, Eckelman B, Vaidyanathan R, Horie T, Fairbairn DJ, Kubo M, Yamagami M, Yamaguchi K, Nishimura M, Uozumi N, et al (2002) Altered shoot/root Na⁺ distribution and bifurcating salt sensitivity in *Arabidopsis* by genetic disruption of the Na⁺ transporter AtHKT1. *FEBS Lett* **531**: 157–161
- Meyer RC, Steinfath M, Lisek J, Becher M, Witucka-Wall H, Törjék O, Fiehn O, Eckardt A, Willmitzer L, Selbig J, et al (2007) The metabolic signature related to high plant growth rate in *Arabidopsis thaliana*. *Proc Natl Acad Sci USA* **104**: 4759–4764
- Milla R, Escudero A, Iriondo JM (2009) Inherited variability in multiple traits determines fitness in populations of an annual legume from contrasting latitudinal origins. *Ann Bot (Lond)* **103**: 1279–1289
- Morrissey J, Baxter IR, Lee J, Li L, Lahner B, Grotz N, Kaplan J, Salt DE, Guerinot ML (2009) The ferroporin metal efflux proteins function in iron and cobalt homeostasis in *Arabidopsis*. *Plant Cell* **21**: 3326–3338
- Philippar K, Fuchs I, Luthen H, Hoth S, Bauer CS, Haga K, Thiel G, Ljung K, Sandberg G, Bottger M, et al (1999) Auxin-induced K⁺ channel expression represents an essential step in coleoptile growth and gravitropism. *Proc Natl Acad Sci USA* **96**: 12186–12191
- Poirier Y, Bucher M (2008) Phosphate transport and homeostasis in *Arabidopsis*. In *The Arabidopsis Book*. American Society of Plant Biologists, Rockville, MD, doi/10.1199/tab.0024, <http://www.aspb.org/publications/arabidopsis/>
- Pyo Y, Gierth M, Schroeder JJ, Cho MH (2010) High-affinity K⁺ transport in *Arabidopsis*: AtHAK5 and AKT1 are vital for seedling establishment and postgermination growth under low K⁺ conditions. *Plant Physiol* **153**: 863–875
- Rauh L, Basten C, Buckler S IV (2002) Quantitative trait loci analysis of growth response to varying nitrogen sources in *Arabidopsis thaliana*. *Theor Appl Genet* **104**: 743–750
- Rengel Z, Damon PM (2008) Crops and genotypes differ in efficiency of potassium uptake and use. *Physiol Plant* **133**: 624–636
- Reymond M, Pieper B, Barbier H, Ihnatowicz A, El-Lithy M, Vreugdenhil D, Koornneef M (2007) Genetic and molecular analysis of growth responses to environmental factors using *Arabidopsis thaliana* natural variation. In JHJ Spiertz, PC Struik, HH van Laar, eds, *Scale and Complexity in Plant Systems Research: Gene-Plant-Crop Relations*, Wageningen UR Frontis Series, Vol 21. Springer, Dordrecht, The Netherlands, pp 3–13
- Reymond M, Svistoonoff S, Loudet O, Nussaume L, Desnos T (2006) Identification of QTL controlling root growth response to phosphate starvation in *Arabidopsis thaliana*. *Plant Cell Environ* **29**: 115–125
- Rus A, Baxter I, Muthukumar B, Gustin J, Lahner B, Yakubova E, Salt DE (2006) Natural variants of AtHKT1 enhance Na⁺ accumulation in two wild populations of *Arabidopsis*. *PLoS Genet* **2**: e210
- Ryan PR, Delhaize E, Jones DL (2001) Function and mechanism of organic anion exudation from plant roots. *Annu Rev Plant Physiol Plant Mol Biol* **52**: 527–560
- Sano T, Becker D, Ivashikina N, Wegner LH, Zimmermann U, Roelfsema MR, Nagata T, Hedrich R (2007) Plant cells must pass a K⁺ threshold to re-enter the cell cycle. *Plant J* **50**: 401–413
- Schauer N, Semel Y, Balbo I, Steinfath M, Reipsilber D, Selbig J, Pleban T, Zamir D, Fernie AR (2008) Mode of inheritance of primary metabolic traits in tomato. *Plant Cell* **20**: 509–523
- Schwarz G (1978) Estimating the dimension of a model. *Ann Stat* **6**: 461–464
- Shirvani T, Samedova A, Jangirova S, Salayeva K, Piriye V, Huseinova N (2001) Adaptive strategy of plants for survival under N, P, K limitation. In WJ Horst, MK Schenk, A Bürkert, N Claassen, H Flessa, WB Frommer, H Goldbach, H-W Olfs, V Römheld, B Sattelmacher, U Schmidhalter, S Schubert, NV Wirén, L Wittenmayer, eds, *Plant Nutrition*. Kluwer Academic Publishers, Dordrecht, The Netherlands, pp 170–171
- Sinclair TR (1992) Mineral nutrition and plant growth response to climate change. *J Exp Bot* **43**: 1141–1146
- Sulpice R, Pyl ET, Ishihara H, Trenkamp S, Steinfath M, Witucka-Wall H, Gibon Y, Usadel B, Poree F, Piques MC, et al (2009) Starch as a major integrator in the regulation of plant growth. *Proc Natl Acad Sci USA* **106**: 10348–10353
- Svistoonoff S, Creff A, Reymond M, Sigoillot-Claude C, Ricaud L, Blanchet A, Nussaume L, Desnos T (2007) Root tip contact with low-phosphate media reprograms plant root architecture. *Nat Genet* **39**: 792–796
- Tisné S, Reymond M, Vile D, Fabre J, Dauzat M, Koornneef M, Granier C (2008) Combined genetic and modeling approaches reveal that epidermal cell area and number in leaves are controlled by leaf and plant developmental processes in *Arabidopsis*. *Plant Physiol* **148**: 1117–1127
- Tocquin P, Corbesier L, Havelange A, Pieltain A, Kurtem E, Bernier G, Périlleux C (2003) A novel high efficiency, low maintenance, hydroponic system for synchronous growth and flowering of *Arabidopsis thaliana*. *BMC Plant Biol* **3**: 2
- Torii KU, Mitsukawa N, Oosumi T, Matsuura Y, Yokoyama R, Whittier RE, Komeda Y (1996) The *Arabidopsis ERECTA* gene encodes a putative receptor protein kinase with extracellular leucine-rich repeats. *Plant Cell* **8**: 735–746
- Ungerer MC, Halldorsdottir SS, Modliszewski JL, Mackay TF, Purugganan MD (2002) Quantitative trait loci for inflorescence development in *Arabidopsis thaliana*. *Genetics* **160**: 1133–1151
- Van Ooijen JW (2004) MapQTL®5, Software for mapping of quantitative loci in experimental populations. Kyazma B.V., Wageningen, The Netherlands
- van Zanten M, Snoek LB, Proveniers MCG, Peeters AJM (2009) The many functions of ERECTA. *Trends Plant Sci* **14**: 214–218
- Véry AA, Sentenac H (2003) Molecular mechanisms and regulation of K⁺ transport in higher plants. *Annu Rev Plant Biol* **54**: 575–603
- Vijayraghavan V, Soole K (2010) Effect of short- and long-term phosphate stress on the non-phosphorylating pathway of mitochondrial electron transport in *Arabidopsis thaliana*. *Funct Plant Biol* **37**: 455–466
- Viola R, Davies HV (1992) A microplate reader assay for rapid enzymatic quantification of sugars in potato tubers. *Potato Res* **35**: 55–58
- Vreugdenhil D, Aarts MGM, Koornneef M, Nelissen H, Ernst WHO (2004) Natural variation and QTL analysis for cationic mineral content in seeds of *Arabidopsis thaliana*. *Plant Cell Environ* **27**: 828–839
- Wang Y, Wu WH (2010) Plant sensing and signaling in response to K⁺-deficiency. *Mol Plant* **3**: 280–287
- Ward JT, Lahner B, Yakubova E, Salt DE, Raghothama KG (2008) The effect of iron on the primary root elongation of *Arabidopsis* during phosphate deficiency. *Plant Physiol* **147**: 1181–1191
- Waters BM, Grusak MA (2008) Quantitative trait locus mapping for seed mineral concentrations in two *Arabidopsis thaliana* recombinant inbred populations. *New Phytol* **179**: 1033–1047
- Williamson LC, Ribrioux SPCP, Fitter AH, Leyser HMO (2001) Phosphate availability regulates root system architecture in *Arabidopsis*. *Plant Physiol* **126**: 875–882



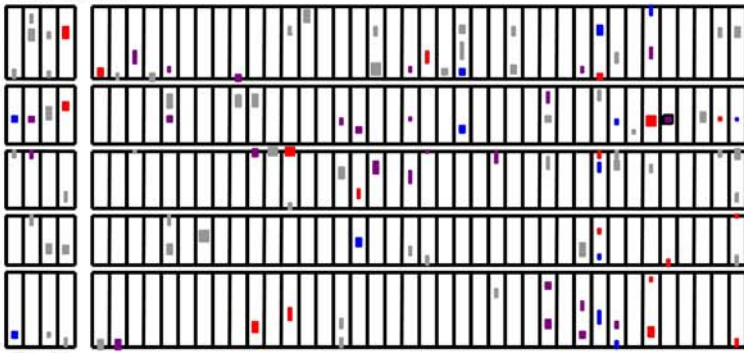
Supplemental Figure S1: Correlations of the selected predictors for the growth related traits.

The graphics show the correlations between the selected predictors for each growth-related trait under the three different nutrient regimes (Control, K-, P-) and for the responses to the K- and P-regimes. Selected predictors are represented by full, black circles. Thin lines and bold lines represent significant correlations between the predictors ($0,001 < P\text{value} < 0,05$ and $P\text{value} < 0,001$, respectively).

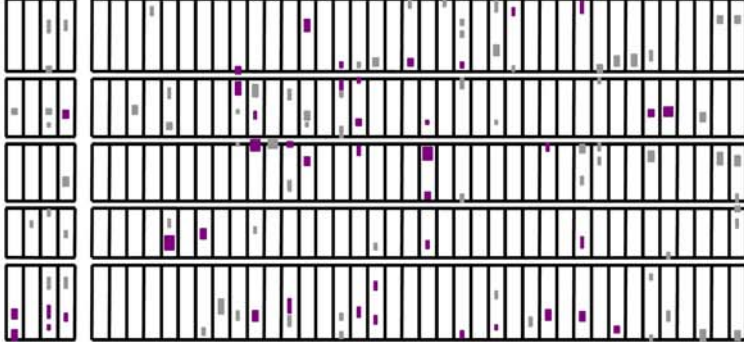


Supplemental Figure S1 (continued): Correlations of the selected predictors for the growth related traits. The graphics show the correlations between the selected predictors for each growth-related trait under the three different nutrient regimes (control, K-, P-) and for the responses to the K- and P-regimes. Selected predictors are represented by full, black circles. Thin lines and bold lines represent significant correlations between the predictors ($0,001 < P\text{value} < 0,05$ and $P\text{value} < 0,001$, respectively).

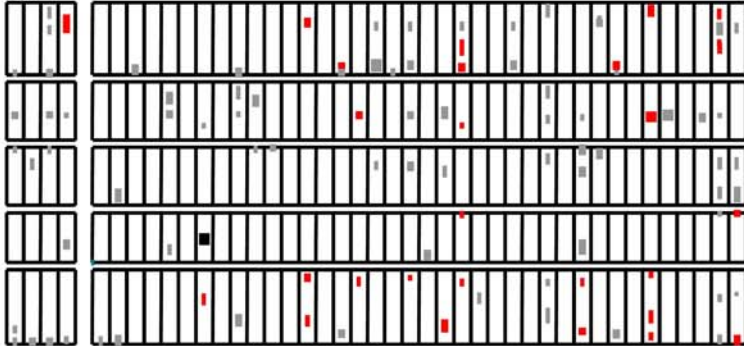
A: Control



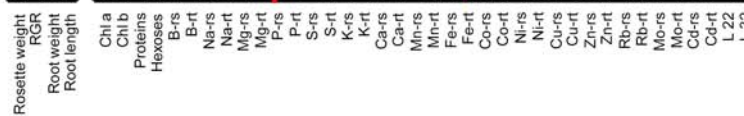
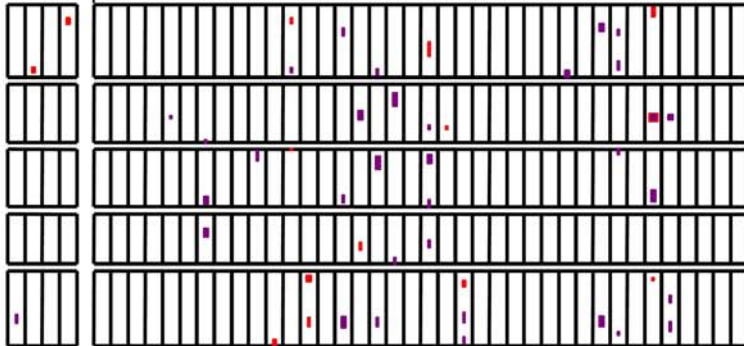
B: K-



C: P-



D: Responses to P- and K-



Supplemental Figure S2: QTL mapping for growth related traits (rosette weight, relative growth rate "RGR", root weight and root length), for chlorophyll (Chla, Chlb)-, protein-, hexose-, ionic traits (for rosette "rs" and root "rt" tissue) and for leaf number at 22DAT (L22) and 32DAT (L32).

The five chromosomes of *A. thaliana* are represented on the left of each panel (top of chromosome 1 on the top and bottom of chromosome 5 at the bottom of each panel). The genetic position of the markers used to elaborate the genetic map are reported by horizontal bars on each chromosome.

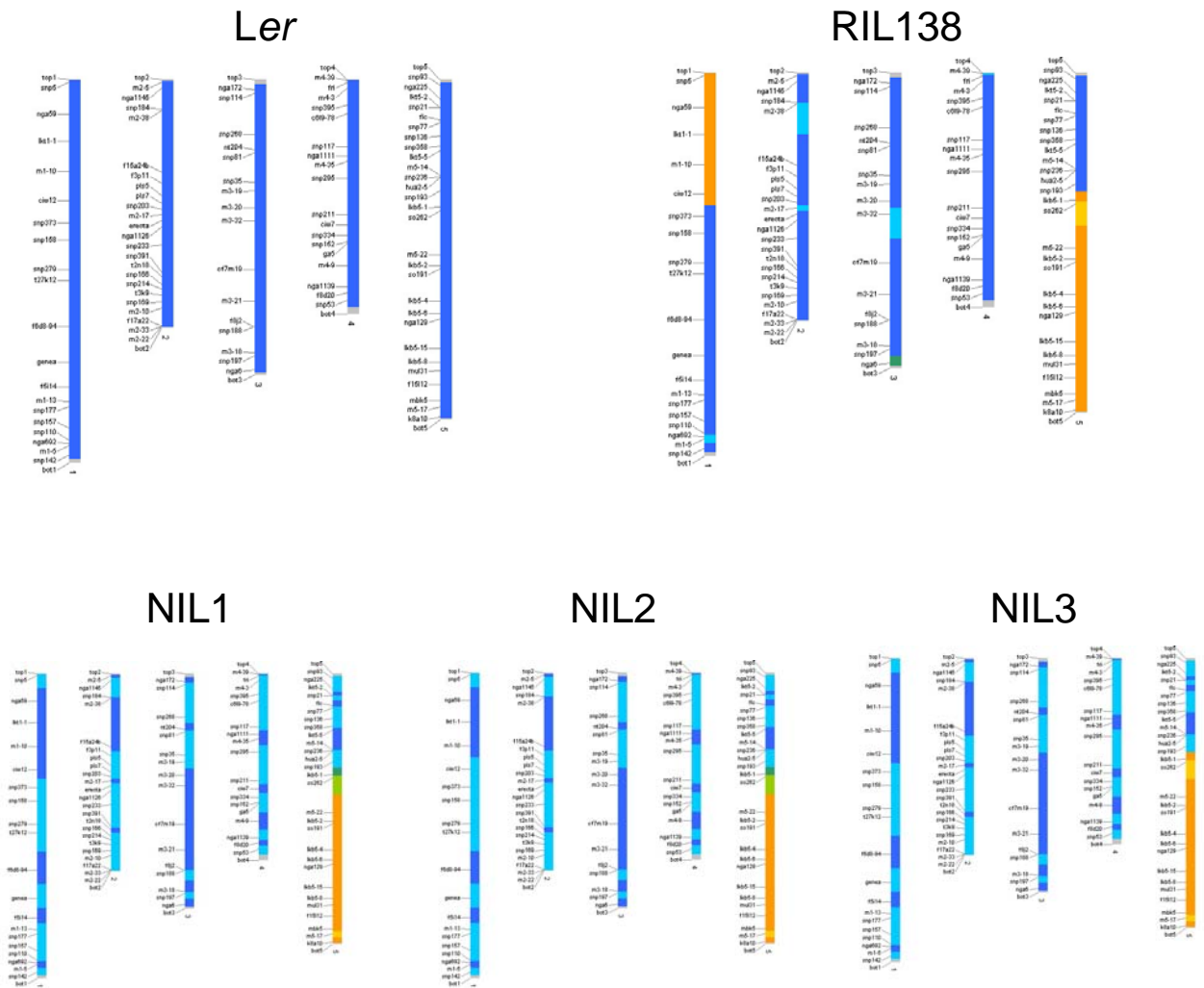
The length of the QTL was determined according to an LOD -1 support interval. QTL with different R^2 (% of explained variance) are reported in different width (see legend). More detailed characterization of these QTL are indicated in the supplemental table S1.

A: QTL detection for the traits quantified in the control hydroponic solution. The QTL model obtained for each trait was then tested for QTL x E significance (see Materials and Methods): Lilac and red QTL indicate that a significant different effect was detected between control and K- and between control and P- conditions, respectively. QTL reported in blue indicates that a significant different effect of this QTL was detected between control and both K- and P- conditions.

B: QTL detection for each trait quantified in the K- hydroponic solution. In lilac are the QTL with significant different effect between K- and control conditions.

C: QTL detection for each trait quantified in the P- hydroponic solution. In red are the QTL with significant different effect between P- and control conditions.

D: QTL detection for the response (see Materials and Methods) of each trait to K- (in lilac) and to P- (in red) conditions.



Supplemental Figure S3: Graphic presentation of the genotypes of Ler, RIL138 and the NILs

The graphic shows the physical map (of the five Arabidopsis chromosomes) with indicated marker positions of Ler, RIL138 and the NIL1, NIL2 and NIL3. The different alleles at the marker positions are color coded: Ler alleles are indicated in blue, Kas-2 alleles in orange and heterozygote alleles in green. Dark blue/orange colors represent tested marker positions and light blue/orange represent the assumed genotype at the respective marker positions according to flanking markers. The tested markers for chromosome 1 are: lkt1-1, NGA59, M1-10, CIW12, F6D8-94, F5I14, NGA692, M1-5; for chromosome 2 are: M2-5, M2-38, F15A24b, M2-17, T2N18, M2-33; for chromosome 3: NGA172, nt204, M3-20, M3-32, CF7M19, M3-21, F8J2, M3-18, NGA6; for chromosome 4: M4-39, NGA1111, M4-35, CIW7, M4-9, F8D20; for chromosome 5: lkt5-2, FLC, lkt5-5, M5-14, lkb5-1, M5-22, lkb5-2, SO191, lkb5-4, lkb5-6, NGA129, lkb5-15, lkb5-8, MUL3-1, F15L12, mbk5, K8A10.

QTL	QTL						QTL	QTL						QTL	QTL						QTL									
	Chromosome	Marker	Position (cM)	Position (Mbp)	LOD	% Expl.		Chromosome	Marker	Position (cM)	Position (Mbp)	LOD	% Expl.		Chromosome	Marker	Position (cM)	Position (Mbp)	LOD	% Expl.		Chromosome	Marker	Position (cM)	Position (Mbp)	LOD	% Expl.			
22DAT	1	SNP11	11.2	11.2	11.2	11.2	1	SNP11	11.2	11.2	11.2	11.2	1	SNP11	11.2	11.2	11.2	11.2	1	SNP11	11.2	11.2	11.2	11.2	1	SNP11	11.2	11.2	11.2	11.2
32DAT	1	SNP11	11.2	11.2	11.2	11.2	1	SNP11	11.2	11.2	11.2	11.2	1	SNP11	11.2	11.2	11.2	11.2	1	SNP11	11.2	11.2	11.2	11.2	1	SNP11	11.2	11.2	11.2	11.2
...

Supplemental Table S1: List of all detected QTL

QTL for rosette weight, relative growth rate (RGR), root weight, root length and total chlorophyll- (Chl a,b), protein and hexose-content in the rosette, as well as ion-content in the rosette (-rs) and the root (-rt) and leaf number at 22DAT and 32DAT (L22, L32) are reported. QTL were detected for each trait in each nutritional regime (control, K- and P-) and for the response to reduced potassium (K response) and reduced phosphate (P response) conditions. The heritability (h^2), position of the closest marker with the highest LOD-score (in cM and Mbp), LOD-score, explained variance (% Expl.; R^2) and additive effect (Additive; 2a) is given (if the additive effect is positive, the *Ler* allele increases the trait value).

marker name	chromosome	phys. pos (Mbp)	forward seq	reverse seq	enzyme for CAPS	annealing temperature
lkt1-1	1	4.9	CAAATCATCCATATGGCAAAGC	CTAGAGCCTCCCACCATGAC	-	60°C
lkt5-2	5	2.19	CAAGAAGGCCGAGAATGAATAG	GTATGAGCCACTATGCCTTGTG	-	60°C
lkt5-5	5	5.62	GAAAAGGCAAGGGAAAG	GCTGCCGTCACCAAAG	-	55°C
lkb5-1	5	10.1	GAAGAGGATTTGTGTGGTG	GTTTGTCAAGGTATTTGGATG	-	55°C
lkb5-2	5	14.8	GGAACGGTATTGAGAATGAAC	CGTGGCAAATAATGGAGAG	-	55°C
lkb5-4	5	17.6	CTGAGCATGTGTTAGTCCTG	CAAACACCACAACAATTCAC	-	55°C
lkb5-6	5	18.6	GAGGTCCTTTATTATTCGC	CTTACCACACAACCAGC	-	50°C
lkb5-8	5	22.4	CTCAATCTCGATCCTACACC	CTCTCTTCTTGCTTATACTG	-	55°C
lkb5-15	5	21.3	CTCGTTTTCCCGCCATTTC	GCTCCACCGATCAAATGTC	Hinf I	55°C

Supplemental Table S2: Primers designed for genotyping of the near isogenic lines. The primers were designed to be used as SSLP marker or CAPS marker to genotype the NILs presented in Figure 2. The table lists the position of the polymorphism (in Mbp), the primer sequence, the restriction enzyme (for the CAPS marker) and the annealing temperature of the primer pairs.